Received: 17 April 2020 | Revised: 24 July 2020 | Accepted: 24 August 2020

DOI: 10.1111/exd.14185

REGULAR ARTICLE

Experimental Dermatology WILEY

Stratum corneum lipidomics analysis reveals altered ceramide profile in atopic dermatitis patients across body sites with correlated changes in skin microbiome

Hila Emmert[1] | Hansjörg Baurecht[1,2] | Frederieke Thielking[1] | Dora Stölzl[1] | Elke Rodriguez[1] | Inken Harder[1] | Ehrhardt Proksch[1] | Stephan Weidinger[1]

[1]Department of Dermatology, Allergology and Venereology, University Hospital Schleswig-Holstein, Kiel, Germany

[2]Department of Epidemiology and Preventive Medicine, University of Regensburg, Regensburg, Germany

Correspondence
Hila Emmert, Department of Dermatology, Venereology and Allergy, University Hospital Schleswig-Holstein, Campus Kiel, Rosalind-Franklin Str. 7, 24105 Kiel, Germany.
Email: hemmert@dermatology.uni-kiel.de

Funding information
The funding sources had no involvement in the study design, the collection, analysis and interpretation of data, the writing of the report and in the decision to submit the article for publication.
The project received infrastructure support through the DFG Cluster of Excellence "Inflammation at Interfaces" (grants EXC306 and EXC306/2 and GE 2879/2-1) and was supported by the German Federal Ministry of Education and Research (BMBF) within the framework of the e:Med research and funding concept (sysINFLAME, grant # 01ZX1306A). S.W is coordinator of the European Union Horizon 2020-funded BIOMAP Consortium (http://www.biomap-imi.eu/) and a co-principal investigator of the German Atopic Eczema Registry (TREATgermany). He has performed consultancies and/or lectured for Sanofi-Genzyme, Regeneron, LEO Pharma, Janssen, Abbvie, Eli Lilly, Pfizer, Novartis, Incyte, Kymab.; and is involved in performing clinical trials with many pharmaceutical industry companies that manufacture drugs used for the treatment of psoriasis and atopic eczema.

Abstract

Background: Atopic dermatitis (AD) is driven by the interplay between a dysfunctional epidermal barrier and a skewed cutaneous immune dysregulation. As part of the complex skin barrier dysfunction, abnormalities in lipid organization and microbiome composition have been described. We set out to systematically investigate the composition of the stratum corneum lipidome, skin microbiome and skin physiology parameters at three different body sites in patients with AD and healthy volunteers.

Methods: We analysed tape strips from different body areas obtained from 10 adults with AD and 10 healthy volunteers matched for *FLG* mutation status for 361 skin lipid species using the Metabolon mass spectrometry platform. 16S rRNA data were available from all probands.

Results: Our study showed that the lipid composition differs significantly between body sites and between AD patients and healthy individuals. Ceramide species NS was significantly higher in AD patients compared to healthy volunteers and was also higher in AD patients with a *FLG* mutation compared to AD patients without a *FLG* mutation. The correlation analysis of skin lipid alterations with the microbiome showed that Staphylococcus colonization in AD is positively correlated with ceramide subspecies AS, ADS, NS and NDS.

Conclusion: This is the first study to reveal site-specific lipid alterations and correlations with the skin microbiome in AD.

KEYWORDS

Atopic dermatitis, Filaggrin, lipidome, metabolomics

Hila Emmert and Hansjörg Baurecht are Co-first author.

1 | INTRODUCTION

Several pathophysiological mechanisms are thought to contribute to AD, but the two key drivers are a dysfunctional epidermal barrier and exaggerated type 2 T helper cell (TH2)-mediated immune responses. The two major epidermal barrier structures are the *stratum corneum* intercellular lipid lamellae and tight junction proteins in the nucleated epidermis. The function of the *Stratum corneum* critically depends on proper differentiation of keratinocytes and a coordinated activity of acid, lipid and enzyme constituents. In AD, epidermal barrier dysfunction is consistently observed in affected and unaffected skin and evidenced by elevated markers of epidermal permeability including elevated transepidermal water loss (TEWL),[1] elevation of pH,[2] increased permeability,[3] reduced water retention[4,5] and enhanced susceptibility to infection.[6,7] At the molecular abundance, a reduced expression of epidermal structural proteins such as filaggrin,[8,9] imbalances in protease-protease inhibitor interactions,[10,11] a reduced expression of tight junction proteins[12,13] and an altered skin microbiome configuration[14] has been reported for both lesional and non-lesional skin. Further, several studies have also suggested that skin lipid metabolism, especially ceramide metabolism, is altered in AD. In particular, the chain length of ceramide-linked fatty acids was reported to be decreased,[8,15-17] and it was shown that the lipid chain length reduction correlates with a compromised lipid envelope and thus an impaired barrier function.[16-18] More recently, shifts in the epidermal lipid composition have been reported to correlate with increased *Staphylococcus aureus* colonization.[19] Specifically, abundances of very long-chain ceramides (CER[EOH] C60 and CER[EOH]C68) were higher in AD patients without S *aureus* colonization as compared to AD patients with S. aureus colonization.[19]

Alterations of single or multiple factors impacting barrier function can be mediated through primary mechanisms such as mutations in the gene encoding filaggrin (*FLG*) or indirectly through type 2 immune activity in the skin causing a secondary downregulation of skin barrier genes and stratum corneum lipids. It has been previously shown that knock-down of *FLG* in skin models leads to increased expression of secretory phospholipase A2, which converts phospholipids into fatty acids. In turn, free fatty acids accumulate and contribute to less ordered intercellular lipid lamellae and higher permeability in *FLG* knock-down skin constructs.[20] However, whether filaggrin is indeed responsible for impaired lipid organization remains unclear, as several studies found no correlation between lipids and *FLG* mutations.[16,21,22]

We here set out to systematically analyse the epidermal lipid composition at different body sites and in AD as compared to matched healthy individuals. We further took advantage of existing 16S data to evaluate its potential impact on the skin microbiome composition. To this end, we measured 361 skin lipid species at three different sites, namely the forehead (FH), the cubital fossa (CF) and the proximal lower forearm (LA) in 4 different groups matched for age, sex, presence/absence of AD and presence/absence of *FLG* haploinsufficiency.

2 | METHODS

2.1 | Study population

The study population has been described previously[23] and consisted of four groups of German adults recruited through the POPGEN population-based cohort[24]: (a) subjects with AD carrying a single *FLG* mutation (AD FLGmut), (b) subjects with AD without *FLG* mutations (AD FLGwt), (c) subjects with no history of chronic skin or allergic disorders carrying a single *FLG* mutation (controls FLGmut) and (d) subjects with no history of chronic skin or allergic disorders without *FLG* mutations (controls FLGwt). *FLG* mutation status was available from prior studies.[25] Characteristics of the probands are reported in Table S1. The follow-up examination included a skin examination by an experienced dermatologist blinded to the genotype. AD was defined by the American Academy of Dermatology diagnostic criteria.[26] The selected individuals per group were matched by age and sex, and selected AD patients had to display at least one unaffected antecubital crease. None of the participants had received systemic immunosuppressants or systemic antibiotics in the preceding 3 months. All participants were asked to avoid bathing and application of any topical agent 24 hours prior to the examination visit. All skin biophysical measurements were done in standardized environmental conditions (room temperature, 22 to 25°C; humidity abundances, 30% to 35%). Skin pH was measured with a Skin-pH-Meter® PH 905 (Courage & Khazaka Electronic, Cologne, Germany), and TEWL was measured with the Biox Aquaflux AF200 closed condenser chamber device (Biox Systems Ltd, London, UK) according to international guidelines.[27] The mean of 3 separate measurements was used for analysis.

The study was approved by the ethical review board of the Medical Faculty of the University Kiel, Germany, and written informed consent was obtained from all study participants.

2.2 | Lipid analysis

A total of 348 ceramides (CER), 12 free fatty acids (FFA) and cholesterol sulphate were determined by SFC-MS/MS using the TrueMass® Stratum Corneum Metabolon Lipid Panel (Waters Corporation, Milford, MA/Sciex, Framingham, MA; Metabolon, Inc, Durham, NC) at three body sites (CF, FA and LA).

Four consecutive tape strips were taken using the D-squame pressure instrument from non-lesional skin sites, frozen and stored at −80°C prior analysis. We obtained a total of 60 samples consisting of four pooled D-Squame discs per subject and sampling site. All D-Squame discs were extracted in a batch together with four additional negative control samples using a polar and a non-polar organic solvent after addition of a known amount of surrogate standard solution (C16 ceramide-d31 ((S(C18)16:0)-d31), cis-10-heptadecenoic acid (FA17:1n7) and cholesteryl sulphate-d7). The organic extracts are combined and evaporated to dryness. The dried extract is reconstituted, and an aliquot is analysed on a Waters UPC2/Sciex

QTrap 5500 mass spectrometer SFC-MS/MS system in MRM mode using characteristic parent-fragment mass transitions for each analyte trace.

The semi-quantitative determination of the individual analytes is based on their peak area comparison with the peak areas of their corresponding surrogate standards for which concentrations are known. C16 ceramide-d31 is used as surrogate standard for all ceramides, all fatty acids are referenced to cis-10-heptadecenoic acid, and cholesteryl sulphate is referenced to cholesteryl sulphate d7. Concentrations are given in pmol/disc for individual analytes and each lipid class. Additionally, the per cent composition of individual ceramide subtypes of the ceramide fraction is listed for each sample. Data quality was assessed by precision evaluation based on the median % coefficient of variance (CV) of all analytes in the QC samples. The observed median %CV of 12.2% is less than half of the targeted acceptance criteria for QC precision: median %CV of 25.0%.

2.3 | 16S rRNA gene data processing

Skin samples were subjected to 16S rRNA amplicon sequencing of the hypervariable regions V1 and V2 as described previously.[23] In summary, bacterial genomic DNA was extracted using the PowerSoil DNA Isolation Kit (MoBio Laboratories, Carlsbad, Calif) and the hypervariable regions V1 and V2 of 16S rRNA gene were sequenced on the MiSeq platform (Illumina, San Diego, Calif). Stringent demultiplexing was carried out by allowing no mismatches in either index sequence, and a series of quality steps (dereplication, quality trimming, chimera filtering) were applied before resulting OTUs were classified into bacterial taxa.

2.4 | Statistical analysis

All data are represented as mean ± standard deviation unless otherwise indicated. To evaluate differences between groups, we used the Welch test on relative abundance of lipid species, log-transformed pH and $\log_2$-transformed TEWL values. Differences between sites were evaluated by the paired t test. The balance between proportions of lipid classes was calculated by the Shannon index implemented in the "vegan" (v2.4) package. Correlations of taxa of different abundances (eg phylum and genus) were calculated by the spearman correlation coefficient.

Overall correlation between abundances of lipid species and bacterial abundance across all samples was calculated by sparse canonical correlation analysis with feature selection using the R package "mixOmics" (v6.8.5).

All analyses have to be interpreted as exploratory, and presented P-values are unadjusted if not otherwise stated. If adjustment for multiple testing was applied, false discovery rate (fdr) for univariate analysis and the step-down resampling procedure (mvabund package) for multivariate analysis were used and respective P-values are indicated.

All analyses were conducted using R, version 3.3.2 (www.R-project.org).[28]

3 | RESULTS

3.1 | Total abundances of free fatty acids, ceramides and cholesterol sulphate are increased in AD patients

Using the metabolon lipid panel (MLP), a total of 361 skin lipid species were measured, which covered all three lipid classes, namely free fatty acids (FFAs), ceramides (CERs) and cholesterol sulphate. Ceramide subclasses were further categorized into 10 subclasses according to variations in their fatty acid carbon chain and the sphingoid base architecture following classifications by Motta *et al*[29,30] Classification of measured ceramides can be found in Table S10.

Compared to previous reports,[8,9] the MLP covers the most frequent CERs and FFAs present within the stratum corneum accounting for >95% of the CER and >61% of the FFA subclass distribution (Table S2).

Neither age nor sex showed strong correlation with the relative abundance of ceramides, cholesterol sulphate, free fatty acids of the *stratum corneum* of AD patients and healthy subjects (Figure S1, Figure S2, Table S3). Transepidermal water loss (TEWL) at the different body sites was significantly increased at the forehead (FH) compared to the forearm (FA) in both AD patients ($P = .0053$) and healthy individuals ($P = .0039$) (Table S4), which is in accordance with previous studies.[31] However, no association of pH or TEWL was observed with AD or *FLG* deficiency ($0.12 \leq P \leq .70$). In addition, we did not observe a clear association between TEWL and lipids or cholesterol sulphate abundance at all three sites (Figure S3, Figure S4, Table S5).

3.2 | SC lipid composition differs between body sites

To assess which factors are the major components of variance across all samples, we used a hierarchical clustering approach. Analysis of variance showed that samples cluster mainly according to AD vs. control, rather than *FLG* mutation vs. wild type, confirming that AD is the major component of variance across the data (Figure 1). Notably, samples then cluster according to skin sample site: Samples from the FH showed a distinct regulation pattern compared to samples from the lower forearm (LA) or cubital fossa (CF) (Figure S5).

We next investigated the proportion of the lipid classes at the FH, the CF and the proximal LA in healthy individuals. Lipidome analysis uncovered differences in the abundance of the ceramide subclasses NS, NP, NH and AS between the FH and the CF and the FH and the proximal LA (Figure 2A, Table S2, Table S6). A significant abundance difference of AP was also observed between the FH and the CF and of AH between the FH and the proximal LA (Figure 2A).

In contrast, FFA composition was not significantly different between the 3 sites, apart from the saturated fatty acid 24:0, which significantly differed between the FH and the CF and the FH and the proximal LA (Figure 2B).

The distinct differences in CER lipid classes of the FH compared to the LA and the CF could further be shown by the differences in the Shannon index (Table S7). The CER diversity measured by the Shannon index is significantly reduced in AD patients compared to controls at the CF ($P = .0021$) and the proximal LA ($P = .0185$), but not at the FH (Table S7). This corresponds with an increased proportion of the CER subclasses NS, AS and ADS and a decreased proportion of CER subclasses NP, NH and EOS in AD patients (Figure 3) as previously reported.[32]

3.3 | Stratum corneum lipids are altered in AD patients

Increased total FFA abundance was mainly associated with a global upregulation of all FFAs, and no association was found with a significant upregulation of specific FFA proportions. We did not observe an association of AD with FFA proportions (Shannon entropy) or average FFA chain length (Figure S6). However, in line with previous reports at all 3 sites examined, the average CER chain length was lower in AD as compared to healthy individuals ($P = .00049$) (Figures S7-S9).

Detailed analysis of ceramide and FFA class abundance between patients with AD and healthy individuals showed that for ceramides, the abundance of NS class was significantly higher in AD patients, but no differences in FFAs were observed (Figure S10). Among the AD patients, no ceramide subclass was found to be significantly altered in *FLG* mutation carrier vs. non-mutation carrier (Figure S11, Figure S12A). However, abundance of most FFAs was higher in *FLG* mutation carrier than in non-mutation carrier, but only FFA 22.1 and 24.1 were significantly increased (Figure S12B).

3.4 | SC lipid composition between body sites shows significant differences in abundance of ceramide subclasses and abundance of the saturated fatty acid 24:0

As the data showed that both arm sample sites are similar and in order to increasing the power of analysis, we pooled the data of both the

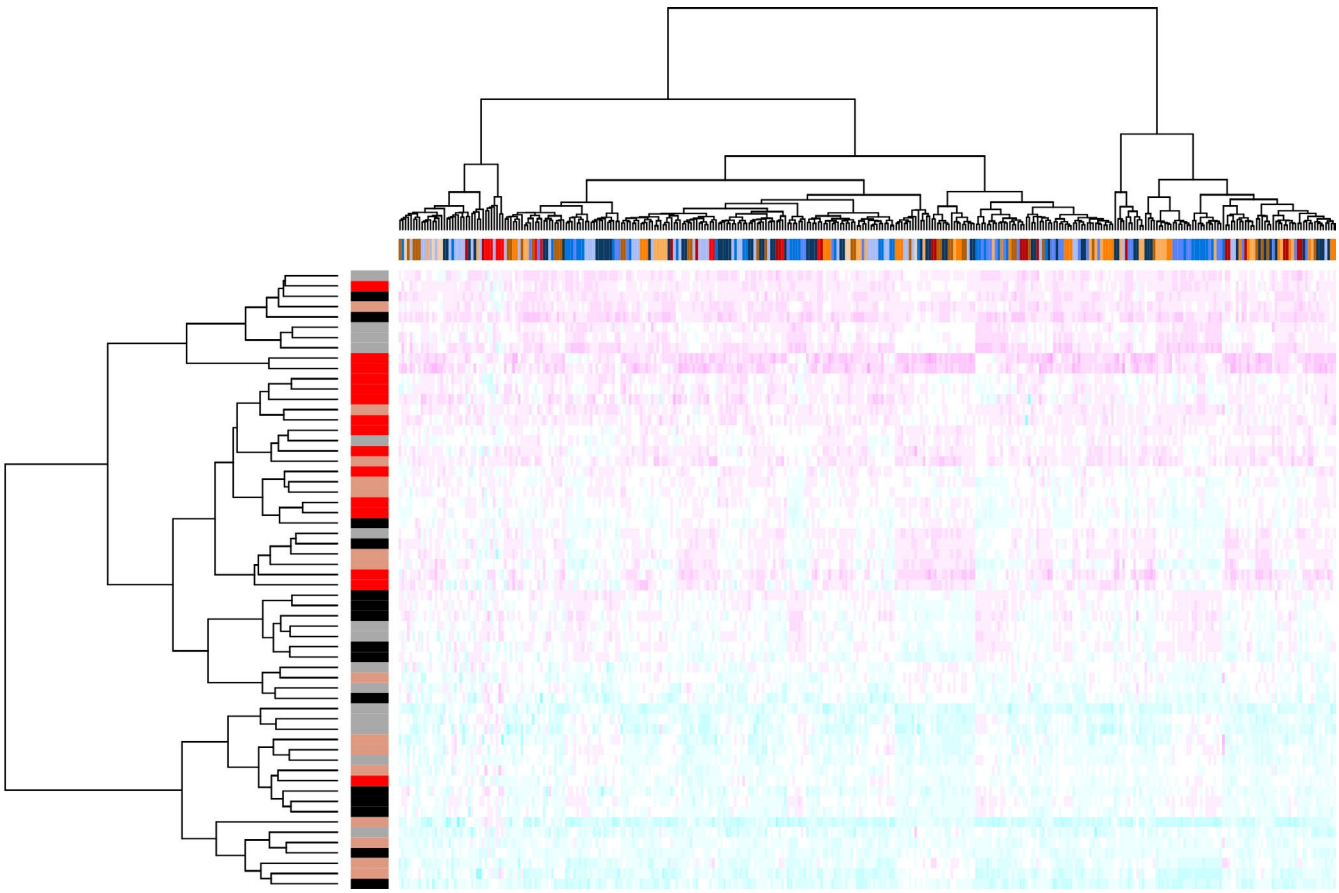

FIGURE 1 Heatmap of ceramides in healthy individuals and patients with AD. The coloured bar at the top indicates ceramide subclass composition. The coloured bar at the side indicates patients with AD with *FLG* mutation (red), patients with AD without *FLG* mutation (orange), healthy individuals without *FLG* mutation (black) and healthy individuals with *FLG* mutation (grey). Hierarchical clustering indicates that FLG is not a major component of variance across data

LA and the CF to generate a forearm (FA) sample group. Differential analysis of the FH and the FA clearly shows that the proportion of CER[NS] and CER[NH] are regulated differently (Figure 4A). Comparison of healthy individuals and AD patients shows that the CER[NS] group is upregulated in the FH in both healthy and AD patients. The observed increase of ceramides in sun exposed areas is in line with previous findings that ceramide production is induced after sun exposure.[33]

The increase of CER[NS] in the FH compared to the FA is greater in healthy individuals than in AD patients, showing that in AD patients there is a reduced induction of ceramide production at the FH (Figure 4). We also detected a site-specific and AD-specific lipid dysregulation in the CER[NH] subclass. The CER[NH] abundance was lower in the FH as compared to the FA. Of note, healthy individuals showed a significantly greater reduction than AD patients (Table S8). These results show that different ceramide subclasses are not only differentially regulated between sites, but that site-specific regulation may differ in AD patients.

To assess whether the site-specific differences in the proportions of the CER subclasses is due to the regulation of all measured ceramides or whether the variance can be explained by a few specific ceramides, we looked at all ceramides in the CER[NS] and CER[NH] group and calculated the p-value, as well as the FDR value of their differential abundance between FH and FA (Figure 4B). Interestingly, only 5 ceramides in both ceramide subclass group were responsible for the site-specific differences in ceramide class proportions. Out of the CER[NS] group, S(C18)16:0, also known as N-(hexadecanoyl)-sphing-4-enine, was the ceramide with the lowest p-value.

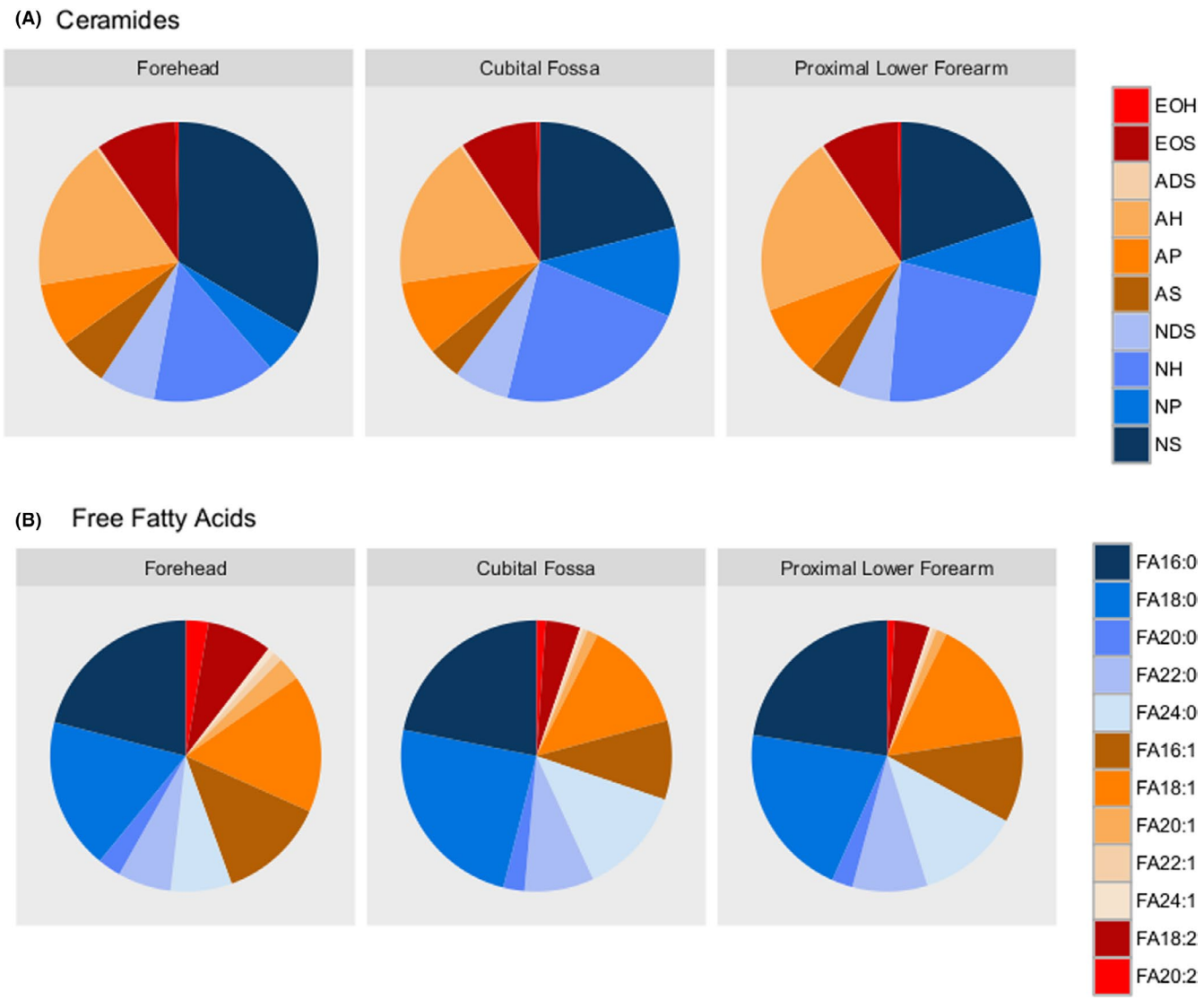

FIGURE 2 Ceramide and free fatty acid distribution in healthy controls at three different sites (A) ceramides: blue = α-hydroxy CERs, red = non-hydroxy CERs and brown/orange = esterified ω-hydroxyl CERs; proportion of CER[NP] is significantly higher in the cubital fossa compared to the forehead, and proportion of CER[AH] is significantly higher in the proximal lower forearm compared to the forehead. (B) Free Fatty Acids: Blue = saturated FFAs, red = MUFAs and brown/orange = DUFAs. Free fatty acid proportions are not significantly altered at the different sites with the exception of saturated fatty acid 24:0, which is significantly increased at the cubital fossa as well as the proximal lower forearm compared to the forehead

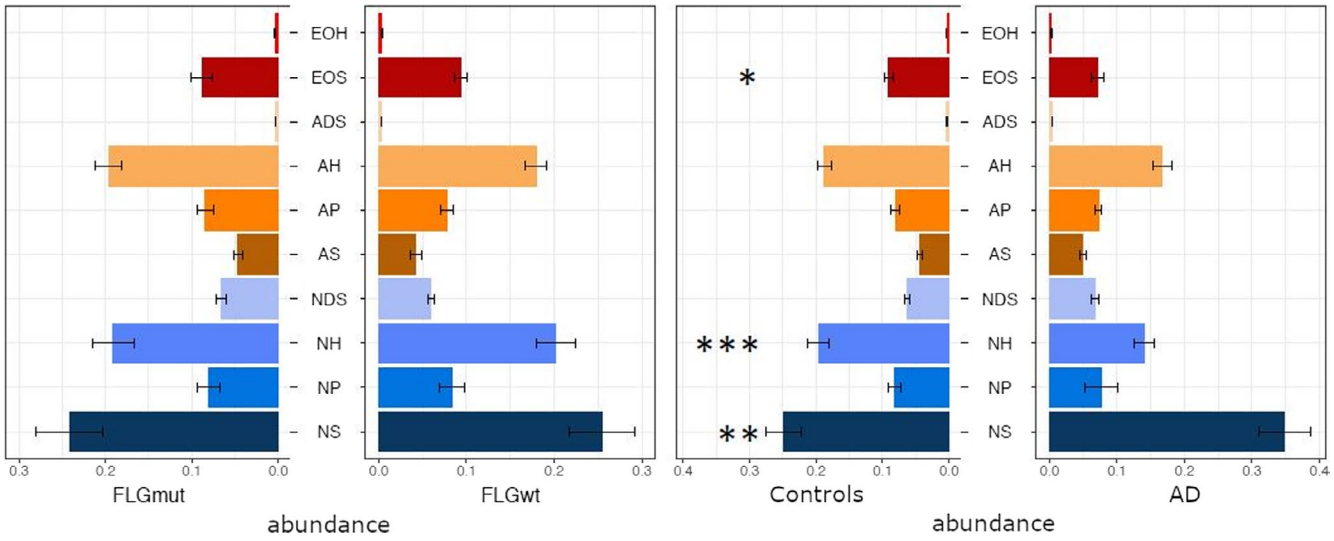

FIGURE 3 Abundance of ceramide classes in AD vs healthy controls and in FLGmut vs FLGwt carriers. Abundance of CER[EOS], CER[NH] and CER[NS] is significantly increased in AD compared to controls. *=$P < .05$, **=$P < .005$, ***=$P < .0005$

S(C18)16:0 has been associated with AD before.[15] In the CER[NH] group, H(C16)26:0 was the ceramide with the lowest p-value.

3.5 | FLG deficiency is not associated with altered stratum corneum lipid composition

Analysis of the lipid class proportions with respect to the presence/absence of *FLG* haploinsufficiency revealed that lipid composition is *FLG* independent. Comparing all *FLG* mutation carriers vs. non-mutation carriers regardless of their AD status, we could not observe significant difference in either ceramide balance or CER subclass proportions at any body site (Table S9). These results are in line with previous reports,[16] where no significant difference in lipid proportions due to *FLG* could be shown. Hierarchical clustering analysis also revealed that *FLG* mutation had no significant impact on sample variability nor on ceramide subclass composition at different sample sites (Figure 1 and Figure S11). There was also no association of FFA average chain length, relative frequencies of specific FFAs or FFA proportions with *FLG* (Figure S6). CER chain length was also not associated with *FLG* at all sample sites (Figures S7-S9).

3.6 | Microbial colonization is shifted towards Staphylococcus in patients with atopic dermatitis

Analysis of the skin microbiome composition at the sites of lipid analysis by 16S sequencing showed a decreased abundance of Bacteroidetes and Actinobacteria and an increased abundance of Firmicutes in AD at all sites (Figure 5A). This is in accordance with previous findings where sampling of separate skin sites showed the same trend.[23] A more detailed analysis revealed a decreased abundance of the genera Chryseobacterium, Propionibacterium and Kocuria and an increased abundance of the genera Staphylococcus and Lactobacillus (Figure 5A), indicating that in AD there is a shift in the bacterial community favouring Staphylococcus and Lactobacillus. A correlation analysis between bacterial and lipid abundances showed a strongly positive correlation of Staphylococcus and ceramide subclasses AS, ADS, NS and NDS in patients with AD, but not in healthy subjects (Table 1). In contrast, the abundances of Propionibacteria, Rothia, Actinomyces, Lactobacillus, Acinetobacter, Haemophilus and Neisseria were negatively correlated with the ceramide species AS, ADS, NS and NDS. In healthy subjects, only Chryseobacteria showed a strong positive correlation with the ceramide species AH, AS and AP, while other bacterial genera showed only weak positive correlations (Table 1). These results indicate a correlation of ceramide species with an increased bacterial colonization with Staphylococcus and a decreased colonization with other bacterial genera in AD, but not in healthy subjects. Further, in AD patients, the abundances of Rothia, Actinomyces, Lactobacillus, Acinetobacter, Haemophilus and Neisseria showed a strongly positive correlation with abundances of saturated short-chain FFAs, such as FA16:0 and FA18:0. The short-chain FFAs FA16:0 and FA18:0 were also negatively correlated with Staphylococcus in AD patients, thus showing both a negative correlation with Staphylococcus in AD and a positive correlation with bacterial genera other than Staphylococcus in healthy volunteers.

4 | DISCUSSION

Our systematic skin lipidome analysis indicates that while across body sites total ceramide, FFA and cholesterol sulphate abundances are increased in AD patients, the relative abundance of several ceramide subclasses (NH, NP, EOS, EOH and EOP) is reduced in AD patients. This might be surprising, as most studies have reported a decrease of ceramides in AD.[34,35] However, decrease of ceramides in AD is due to the decrease of long-chain ceramides with a concomitant increase in short-chain ceramides.[16,35] Out lipid panel did not

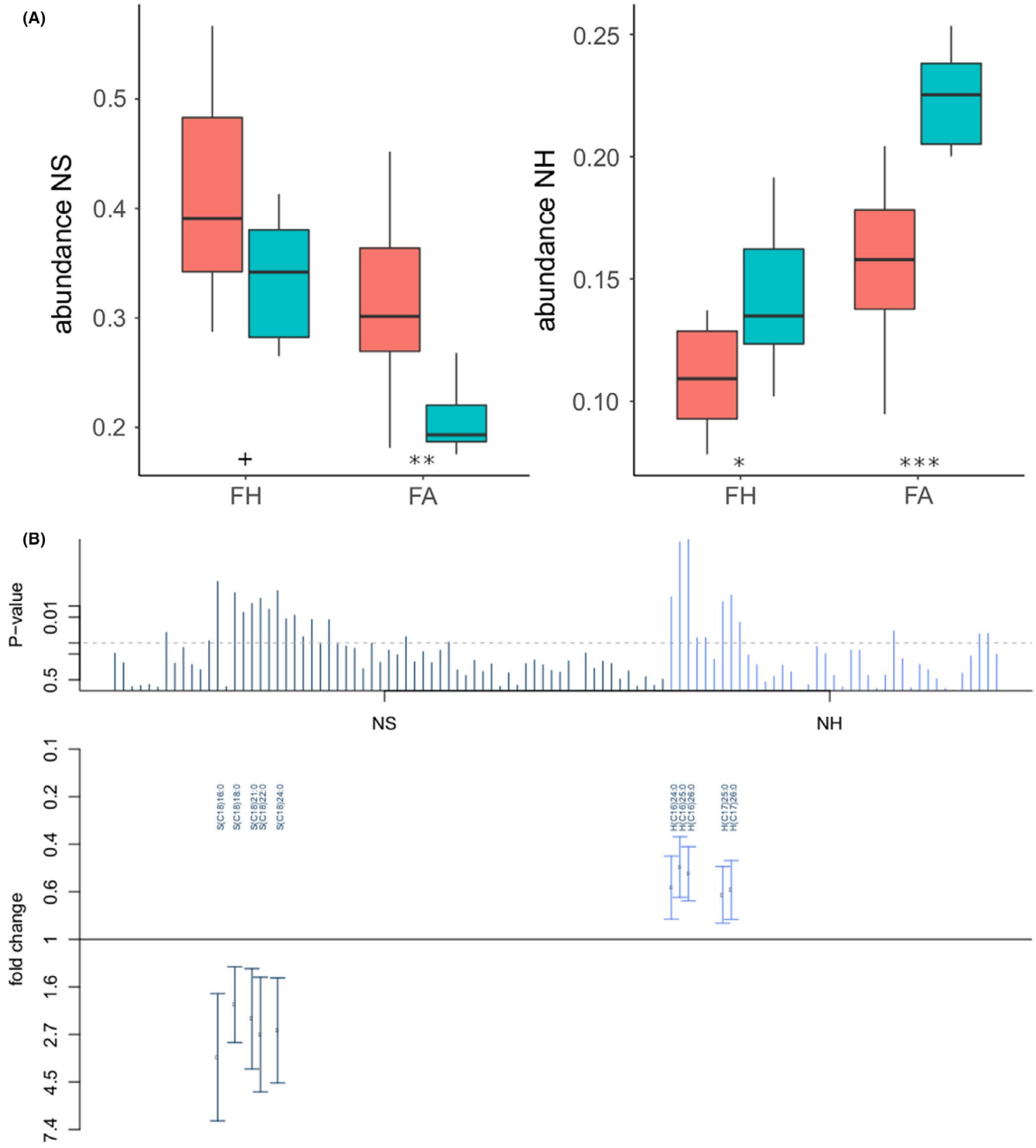

FIGURE 4 Analysis of ceramide subclass composition in healthy individuals and patients with AD across different sample sites. A, Abundance of CER[NS] and CER[NH] in healthy controls and patients with atopic dermatitis at the sun forehead (FH) and the sun arm. Comparison of healthy individuals and AD patients shows that the CER[NS] group is upregulated in the FH in both healthy and AD patients. B, Differential abundance of the single ceramides of the CER[NS] and CER[NH] subclass in healthy controls and patients with atopic dermatitis at forehead (FH) compared to the arm. The fold change is shown for ceramides with a significant false discovery rate. Only 5 ceramides in both ceramide subclass groups were responsible for the site-specific differences in ceramide class proportions. +=$P < .1$, *=$P < .05$, **=$P < .005$, ***=$P < .0005$

cover long-chain ceramides (Figure S10), which explains our finding of increased total ceramide levels as only the increase in short-chain ceramides is detected. In line with previous findings, we also found an increase in the relative abundance of ceramide subclass NS.[17,36] Further, several ceramide species correlated with an increased colonization with Staphylococcus and a decreased colonization

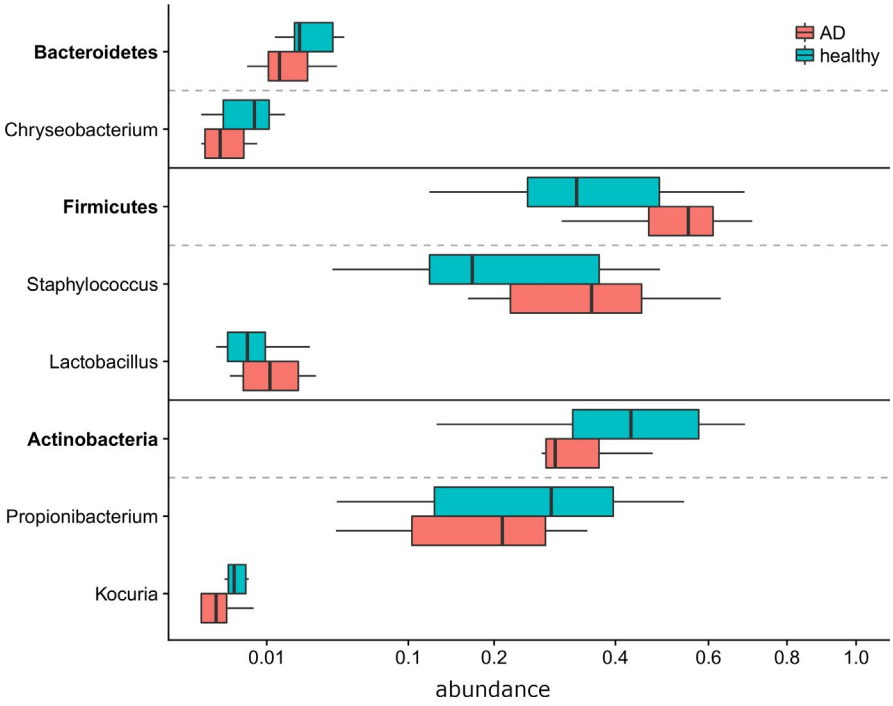

FIGURE 5 Analysis of microbiome core taxa at all skin sample sites. Relative abundance of microbiome core taxa in patients with AD and healthy subjects. In patients with AD, abundance of Bacteroidetes and Actinobacteria is decreased and abundance of Firmicutes increased

with other bacterial genera in AD patients. This is in line with previous reports, which also confirmed an increased colonization of Staphylococcus on the skin of AD patients.[23,37-39] In healthy patients, a positive correlation of Rothia, Actinomyces, Lactobacillus, Acinetobacter, Haemophilus and Neisseria with abundances of saturated short-chain FFAs, such as FA16:0 and FA18:0, was observed, while in AD patients FA16:0 and FA18:0 negatively correlated with Staphylococcus. The short-chain FFAs FA16:0 and FA18:0 thus show an overall inverse correlation effect to bacterial colonization as observed by lipid species correlation. However, this result has to be interpreted with caution, as many topical formulations contain C16:0 and C18:0. While patients were advised to not use any topical treatment for 24 hours before samples were taken, the washout period is short and it is possible that residues of C16:0 and C18:0 remained, which could explain increased levels of C16:0 and C18:0 in AD patients. Additionally, the glue of tape strips often contains C16:0 and C18:0 as well, but as negative samples did not reveal upregulated levels we conclude that the elevated levels of C16:0 and C18:0 were not due to sampling methods. Another concern regarding the interpretation of this data is that the first tape strip could contain high levels of C16:0 and C18:0 from sebum. A recent study analysed the difference in sebum fatty acid profiles in AD patients and concluded that C18 ceramides were decreased in AD patients compared to healthy subjects.[36] Thus, although the correlation of C16:0 and C18:0 levels with skin microbiome changes has to be interpreted with caution, it seems that the elevated levels in AD patients are not due to sampling methods or differences in sebum. It is tempting to speculate that these saturated short-chain FFAs could play an important role in reversing lipid deregulation in AD, but further studies are warranted to analyse beneficial properties of these FFAs.

Our analysis also revealed significant changes between body areas, especially with regard to abundances of ceramide subclasses. The lipid profile at different sites in healthy skin has previously been studied,[40,41] but no analysis of different skin sites in AD has been conducted. Ludovici *et al* could show that sebaceous gland secretion plays a role in lipid composition and that lipid composition differs at different body sites in respect to sebaceous gland density.[41] While NS ceramides are upregulated at the FH in both healthy and AD patients, NH ceramides are downregulated. In both classes, we can see that the site-specific regulation is different between healthy individuals and patients with AD. While the differences in NS class are mainly due to alterations in the abundances of S(C18)16:0, the differences in NH class are primarily due to changes in H(C16)26:0. While S(C18)16:0 is a well-known ceramide already identified to be implicated in AD pathogenesis, the biological role of H(C16)26:0 is still unknown. Further studies will be needed to elucidate the biological function of H(C16)26:0 and the possible implications for the pathogenesis in AD. Analysis of ceramide abundances at the FH shows that ceramide abundances are much more similar between healthy individuals and AD patients, as compared to the FA where ceramide abundances differ more greatly. This indicates a complex dysregulation of skin lipid metabolism in AD, but further studies will be needed to verify our findings.

Other than sebaceous gland density and differences in skin site physiology, filaggrin could also play a role in lipid composition regulation. Filaggrin monomers can be incorporated into the lipid envelope in the stratum corneum, and mutation in *FLG* can thus lead to impaired skin barrier function. One possible mechanism by which *FLG* mutation can lead to altered lipid organization is via secretory phospholipase A2 IIA (sPLA2), which converts phospholipids to fatty

TABLE 1 Analysis of microbiome core taxa at all skin sample sites. Correlation analysis of skin lipids and microbiome core taxa. The abundance of various ceramide species correlated strongly positive with the abundance of Staphylococcus and strongly negative with Propionibacterium and Acinetobacter in AD patients, but not in healthy subjects

	Actinobacteria				Firmicutes				Proteobacteria			
	Controls											
	Propionibacterium	Corynebacterium	Kocuria	Rothia	Staphylococcus	Streptococcus	Anaerococcus	Finegoldia	Acinetobacter	Haemophilus	Neisseria	Chryseobacterium
AH	0.310	0.436	0.026	−0.291	−0.081	−0.087	0.207	0.322	0.424	−0.086	−0.430	0.634
As	***0.407***	***0.471***	−0.033	***−0.154***	***0.060***	0.068	0.391	0.416	***0.389***	***0.118***	***−0.231***	0.387
AP	0.337	0.468	0.019	−0.302	−0.086	−0.084	0.224	0.343	0.452	−0.082	−0.452	0.671
NP	0.179	0.287	0.081	−0.263	−0.063	−0.121	0.126	0.233	0.307	−0.127	−0.350	0.487
FA16:0	***−0.436***	***−0.555***	0.067	***0.260***	***0.089***	−0.010	−0.280	−0.379	***−0.498***	***0.000***	***0.444***	−0.701
FA18:0	***−0.429***	***−0.552***	0.054	***0.272***	***0.090***	0.023	−0.276	−0.381	***−0.500***	***−0.014***	***0.454***	−0.710
FA18:2	0.206	0.095	−0.339	0.320	0.032	0.325	0.101	−0.039	−0.056	0.357	0.265	−0.233
FA20:1	0.586	0.529	−0.490	0.226	−0.023	0.415	0.336	0.226	0.290	0.464	0.021	0.209
FA20:2	***0.631***	***0.622***	−0.430	***0.104***	***−0.049***	0.343	0.372	0.313	***0.404***	***0.387***	***−0.128***	0.403
FA22:1	0.634	0.573	−0.529	0.244	−0.026	0.449	0.364	0.246	0.315	0.501	0.021	0.228
FA24:1	***0.600***	***0.557***	−0.472	***0.189***	***−0.031***	0.393	0.347	0.253	***0.325***	***0.441***	***−0.025***	0.268

	Cases									
	Propionibacterium	Corynebacterium	Actinomyces	Rothia	Staphylococcus	Lactobacillus	Acinetobacter	Haemophilus	Neisseria	Enhydrobacter
AS	***−0.360***	***0.118***	−0.847	***−0.640***	***0.700***	−0.808	***−0.835***	***−0.911***	***−0.706***	−0.477
ADS	−0.357	0.112	−0.887	−0.670	0.723	−0.839	−0.867	−0.944	−0.743	−0.496
NS	−0.370	0.117	−0.902	−0.681	0.738	−0.855	−0.884	−0.963	−0.754	−0.506
NDS	−0.416	0.157	−0.812	−0.617	0.710	−0.803	−0.832	−0.909	−0.669	−0.471
FA16:0	***−0.080***	***0.158***	0.904	***0.661***	***−0.496***	0.680	***0.692***	***0.737***	***0.807***	0.423
FA18:0	***−0.066***	***0.143***	0.853	***0.625***	***−0.474***	0.646	***0.658***	***0.701***	***0.761***	0.402
FA20:0	−0.254	0.240	0.699	0.503	−0.280	0.452	0.454	0.474	0.647	0.292
FA22:0	−0.296	0.267	0.721	0.517	−0.271	0.452	0.453	0.472	0.671	0.295
FA24:0	***−0.232***	***0.241***	0.825	***0.596***	***−0.367***	0.559	***0.564***	***0.593***	***0.755***	0.357
FA20:2	0.184	−0.211	−0.822	−0.596	0.392	−0.576	−0.583	−0.615	−0.747	−0.365
FA24:1	***−0.268***	***0.098***	−0.544	***−0.413***	***0.470***	−0.534	***−0.553***	***−0.604***	***−0.450***	−0.313

≥−0.8	−0.5 ≤ r < −0.8	−0.3 ≤ r < −0.5	−0.1 ≤ r < −0.3	|r| < 0.1	0.1 ≤ r < 0.3	0.3 ≤ r < 0.5	0.5 ≤ r < 0.8	≥0.8

[a]Bold and italic values indicate nominal significant associations ($P<.05$).

acids. In 3D skin constructs, a *FLG* knock-down led to increased activation of sPLA2 and to an accumulation of free fatty acids.[20]

In this study, we have comprehensively profiled lipid species in correlation with the microbiome. We have utilized the non-invasive method of tape stripping to analyse skin lipids in 10 patients with AD and 10 healthy subjects. Although our study cohort is small, we have a balanced study design, and by utilizing the complex lipid panel, we were able to measure all three lipid classes, including ceramides, but also cholesterol sulphate and free fatty acids. Previous studies have already utilized tape stripping and lipidomics analysis to investigate lipid composition in AD.[15] The strength of our study is that we have not only analysed ceramides, but also cholesterol sulphate and free fatty acids. Moreover, to the best of our knowledge we are the first to directly compare the lipid profile at different skin sites in parallel with analysing the microbiome. The limitation of our study is the small study cohort as well as missing longitudinal data to investigate lipid ratios during the disease course. Another limitation of our study that by using a targeted lipidomics approach, we might have not analysed lipids that are of importance (eg very long-chain FFAs or long-chain ceramides).

We conclude that site-specific sampling is important for the holistic analysis of AD lipidomics and that lipid dysregulation in AD is dependent on exogeneous factors.

CONFLICT OF INTEREST

The authors declare that they have no relevant conflicts of interest.

AUTHOR CONTRIBUTIONS

HE, ER, and SW designed the study. FT, DS, and IH performed biosampling. ER performed sample processing and analysis. HE and HB analysed the data and wrote the manuscript. ER, EP and SW revised the manuscript critically.

ORCID

Hila Emmert https://orcid.org/0000-0002-7051-7350
Hansjörg Baurecht https://orcid.org/0000-0002-9265-5594
Elke Rodriguez https://orcid.org/0000-0003-3692-3950
Ehrhardt Proksch https://orcid.org/0000-0002-5816-1822
Stephan Weidinger https://orcid.org/0000-0003-3944-252X

REFERENCES

[1] E. A. Holm, H. C. Wulf, L. Thomassen, G. B. Jemec, *J. Am. Acad. Dermatol.* **2006**, *55*, 772.
[2] S. G. Danby, M. J. Cork, *Curr. Probl. Dermatol.* **2018**, *54*, 95.
[3] H. Ogawa, T. Yoshiike, *Pediatric Dermatol.* **1992**, *9*, 383.
[4] E. Berardesca, D. Fideli, G. Borroni, G. Rabbiosi, H. Maibach, *Acta Derm. Venereol.* **1990**, *70*, 400.
[5] T. Knor, A. Meholjic-Fetahovic, A. Mehmedagic, *Acta Derm. Venerol. Croatica* **2011**, *19*, 242.
[6] S. M. Rangel, A. S. Paller, *Clin. Dermatol.* **2018**, *36*, 641.
[7] S. M. Langan, K. Abuabara, S. E. Henrickson, O. Hoffstad, D. J. Margolis, *J. Investig. Dermatol.* **2017**, *137*, 1375.
[8] J. van Smeden, W. A. Boiten, T. Hankemeier, R. Rissmann, J. A. Bouwstra, R. J. Vreeken, *Biochim. Biophys. Acta* **2014**, *1841*, 70.
[9] t'Kindt R., Jorge L., Dumont E., P. Couturon, F. David, P. Sandra, *Anal. Chem.* **2012**, *84*, 403.
[10] S. Igawa, M. Kishibe, M. Minami-Hori, M. Homma, H. Tsujimura, J. Ishikawa, *J. Investig. Dermatol.* **2017**, *137*, 449.
[11] A. V. Rawlings, R. Voegeli, *Cell Tissue Res.* **2013**, *351*, 217.
[12] A. De Benedetto, N. M. Rafaels, L. Y. McGirt, *J. Allergy Clin. Immunol.* **2011**, *127*, 773.
[13] K. Yoshida, A. Kubo, H. Fujita, M. Yokouchi, K. Ishii, H. Kawasaki, *J. Allergy Clin. Immunol.* **2014**, *134*, 856.
[14] H. H. Kong, J. Oh, C. Deming, S. Conlan, E.A. Grice, M.A. Beatson, *Genome Res.* **2012**, *22*, 850.
[15] E. Berdyshev, E. Goleva, I. Bronova, *JCI Insight* **2018**, *3*, e98006.
[16] C. Tam, J. J. Mun, D. J. Evans, S. M. Fleiszig, *J. Clin. Investig.* **2012**, *122*, 3665.
[17] J. Ishikawa, H. Narita, N. Kondo, M. Hotta, Y. Takagi, Y. Masukawa, *J. Investig. Dermatol.* **2010**, *130*, 2511.
[18] M. Burian, B. Schittek, *Int. J. Med. Microbiol.* **2015**, *305*, 283.
[19] S. Li, M. Villarreal, S. Stewart, J. Choi, G. Ganguli-Indra, D.C. Babineau, *Br. J. Dermatol.* **2017**, *177*, e125.
[20] K. Vavrova, D. Henkes, K. Struver, M. Sochorova, B. Skolova, M.Y. Witting, *J. Investig. Dermatol.* **2014**, *134*, 746.
[21] S. Tyanova, T. Temu, P. Sinitcyn, A. Carlson, M.Y. Hein, T. Geiger, *Nat. Methods* **2016**, *13*, 731.
[22] S. Motta, M. Monti, S. Sesana, R. Caputo, S. Carelli, R. Ghidoni, *Biochim. Biophys. Acta* **1993**, *1182*, 147.
[23] H. Baurecht, M. C. Ruhlemann, E. Rodriguez, *J. Allergy Clin. Immunol.* **2018**, *141*(5), 16681676
[24] U. Nothlings, M. Krawczak, *Gesundheitsforschung Gesundheitsschutz* **2012**, *55*, 831.
[25] L. Paternoster, M. Standl, J. Waage, *Nat. Genet.* **2015**, *47*, 1449.
[26] L. F. Eichenfield, W. L. Tom, S. L. Chamlin, S.R. Feldman, J.M. Hanifin, E.L. Simpson, *J. Am. Acad. Dermatol.* **2014**, *70*, 338.
[27] J. du Plessis, A. Stefaniak, F. Eloff, S. John, T. Agner, T.C. Chou, *Skin Res. Technol.* **2013**, *19*, 265.
[28] R Core Team. A Language and Environment for Statistical Computing. R Foundation for Statistical Computing, Vienna, Austria **2016**.
[29] J. van Smeden, L. Hoppel, R. van der Heijden, T. Hankemeier, R. J. Vreeken, J. A. Bouwstra, *J. Lipid Res.* **2011**, *52*, 1211.
[30] S. S. H. Weng, F. Demir, E. K. Ergin, S. Dirnberger, A. Uzozie, D. Tuscher, *Mol. Cell. Proteomics* **2019**, *18*, 2335.
[31] A. B. Cua, K. P. Wilhelm, H. I. Maibach, *Br. J. Dermatol.* **1990**, *123*, 473.
[32] J. van Smeden, J. A. Bouwstra, *Curr. Probl. Dermatol.* **2016**, *49*, 8.
[33] J. Yao, H. E. Bi, Y. Sheng, R.L. Wendu, C.H. Wang, *Int. J. Mol. Sci.* **2013**, *14*, 10355.
[34] G. Imokawa, A. Abe, K. Jin, Y. Higaki, M. Kawashima, A. Hidano, *J. Investig. Dermatol.* **1991**, *96*, 523.
[35] M. Blaess, H. P. Deigner. *Int. J. Mol. Sci.* **2019**, *20*, 3967.
[36] K. Agrawal, L. A. Hassoun, N. Foolad, K. Borkowski, T.L. Pedersen, *Prostaglandins Leukot. Essent. Fatty Acids* **2018**, *134*, 7.
[37] J. J. Leyden, R. R. Marples, A. M. Kligman, *Br. J. Dermatol.* **1974**, *90*, 525-530.
[38] D. Abeck, M. Mempel, *Br. J. Dermatol.* **1998**, *139*(Suppl 53), 13.
[39] L. Blicharz, L. Rudnicka, Z. Samochocki, *Postepy Dermatol. Alergol.* **2019**, *36*, 11.
[40] J. Mutanu Jungersted, L. I. Hellgren, J. K. Hogh, T. Drachmann, G. B. Jemec, T. Agner, *Acta Derm. Venereol.* **2010**, *90*, 350.
[41] M. Ludovici, N. Kozul, S. Materazzi, R. Risoluti, M. Picardo, E. Camera, *Sci. Rep.* **2018**, *8*, 11500.

SUPPORTING INFORMATION

Additional supporting information may be found online in the Supporting Information section.

Figure S1. Impact of sex on total abundance of ceramides, cholesterol and free fatty acids.

Figure S2. Correlation of age with total abundance of ceramides, cholesterol and free fatty acids.

Figure S3. Correlation of TEWL with total abundance of ceramides, cholesterol and free fatty acids.

Figure S4. Correlation of pH with total abundance of ceramides, cholesterol and free fatty acids.

Figure S5. Heatmap of ceramides in healthy individuals and patients with AD. The colored bar at the top indicates ceramide subclass composition. The colored bar at the side indicates sample site: Forehead (red), forearm (blue), antecubital fossa (darkblue).

Figure S6. Free fatty acid chain length in *FLG*mut and *FLG*wt carrier, as well as in healthy individuals and patients with AD.

Figure S7. Average chain length of CER (left) and FFA (right) at the forehead. Comparison between Ctrl and AD (upper row), FLGwt and FLGmut (middle row) and all 4 study groups (lower row).

Figure S8. Average chain length of CER (left) and FFA (right) at the cubital fossa. Comparison between Ctrl and AD (upper row), FLGwt and FLGmut (middle row) and all 4 study groups (lower row).

Figure S9. Average chain length of CER (left) and FFA (right) at the proximal lower arm. Comparison between Ctrl and AD (upper row), FLGwt and FLGmut (middle row) and all 4 study groups (lower row).

Figure S10. Ceramide (A) and FFA (B) abundance in AD patients vs healthy individuals. (A) and in AD patients with *FLG* mutation carrier vs. non-carrier (B). Significant differences are indicated by (*).

Figure S11. Ceramide abundance in *FLG* mutation carrier vs. non-carrier at three different sites (A) forehead, (B) cubital fossa and (C) proximal lower arm. Blue = α-hydroxy CERs, red = nonhydroxy CERs and brown/orange = esterfied ω-hydroxy CERs.

Figure S12. Ceramide (A) and FFA (B) abundance in AD patients comparing *FLG* mutation carrier vs. non-carrier. Significant differences are indicated by (*).

Table S1. Proband characteristics.

Table S2. Ceramide compsition in healthy volunteers without *FLG* mutations measured by MLP = Metabolon Lipid Panel.

Table S3. Correlation of age and sex on lipid composition

Table S4. TEWL and pH measurements in healthy individuals and patients with AD as well as *FLG* competent and *FLG* deficient individuals. Fh: forehead, Fa: forearm.

Table S5. Correlation of TEWL and pH on lipid composition

Table S6. Ceramide species (pmol/disk) significantly different at a threshold of 0.01 between AD patients and controls in at least one of the three sites: forehead, cubital fossa, proximal lower arm. FC = fold change, CI = confidence interval.

Table S7. Balance of ceramides and free fatty acids measured by the Shannon Index.

Table S8. Differential analysis of CER[NS] and CER[NH] in healthy individuals and patients with AD.

Table S9. Ceramide proportions (relative abundance) and their 95% CIs in FLG wildtype (FLGwt) and FLG mutation carriers (FLGmut).

Table S10. Ceramide anaytes of the Metabolon Lipid Panel.

How to cite this article: Emmert H, Baurecht H, Thielking F, et al. Stratum corneum lipidomics analysis reveals altered ceramide profile in atopic dermatitis patients across body sites with correlated changes in skin microbiome. *Exp Dermatol*. 2021;30:1398–1408. https://doi.org/10.1111/exd.14185